# Mn-doped ScN: A dilute ferromagnetic semiconductor with local exchange coupling

Aditi Herwadkar and Walter R. L. Lambrecht
*Department of Physics, Case Western Reserve University, Cleveland, Ohio 44106-7079, USA*
(Received 28 June 2005; revised manuscript received 21 September 2005; published 27 December 2005)

We present local spin density functional calculations for Mn-doped ScN using the linear muffin-tin orbital method in a supercell approach, including structural relaxation. Mn is found to induce a localized state in middle of the band gap of ScN with $t_{2g}$ character which spin splits and leads to a net magnetic moment of about $2-3\mu_B$ per Mn. The defect is a deep acceptor with 0/- transition state at about 0.5 eV above the Fermi level. The magnetic moment increases when in the negative charge state by acquiring more $e_g$ majority spin electrons and will thus persist even in the presence of the commonly found unintentional background *n*-type doping of ScN. Up to fourth nearest neighbors exchange interactions are found to be ferromagnetic. The experimentally observed high solubility of Mn in ScN, presumably related to their common crystal structure, is favorable for this dilute magnetic semiconductor. Within mean field theory the Curie temperature is estimated to be above 400 K for 3% Mn. While this may be overly optimistic because of the neglect of disorder, the *n*-type character of ScN adds further interest to this unusual magnetic semiconductor because the spin-split conduction bands are nondegenerate and thus essentially free from spin-orbit coupling induced spin relaxation.

DOI: 10.1103/PhysRevB.72.235207 PACS number(s): 75.50.Pp, 71.55.Eq, 75.30.Hx

## I. INTRODUCTION

There is currently great interest in dilute ferromagnetic semiconductors. While Mn-doped GaAs has been well established to have carrier induced ferromagnetic coupling between local magnetic moments on Mn atoms, the maximum Curie temperature obtained after careful annealing treatments is about 150–173 K.[1] In order to avoid precipitation of undesirable MnAs secondary phases, Mn-doped GaAs needs to be grown at low temperatures which may lead to reduced crystalline quality of the semiconductor host. There is clearly an interest in finding an alternative semiconductor host and magnetic dopant combinations with $T_c$ above room temperature. One limitation that is shared by almost all traditional semiconductors tried up to now is that the solubility of transition metal dopants like Mn in them is rather low and this may be assumed to be at least partially due to the different crystal structures of likely precipitate phases and the semiconductor host.

In this paper we propose to overcome this problem by considering a less well-known semiconductor ScN, which has as advantage that it shares the crystal structure with that of the corresponding (antiferro)magnetic compounds: MnN or CrN. In fact, ScN has the simple rocksalt structure while MnN has a very closely related slightly tetragonally distorted rocksalt structure known as the $\theta$ phase.[2] In fact all the early transition metal nitrides ScN, TiN, CrN, and MnN share the rocksalt structure.[3] Their lattice constants are also fairly close. Clearly this should facilitate mutual solubility and alloy formation. Continuous alloys have recently been grown by Al-Brithen *et al.*[4] Unfortunately, however, these authors did not report any magnetic measurements. Although $\theta$ MnN is antiferromagnetic, the calculations reported here show that Mn doped in ScN prefers ferromagnetic coupling. Before we describe these results, we give a brief reminder of ScN properties.

Although ScN has long been thought to be a semimetal,[5] recent advances[6,7] in growing stoichiometrically pure ScN have definitely shown it to be an indirect semiconductor with an indirect band gap of about 1 eV and a first strong direct transition at about 2 eV. While early ScN had carrier concentrations of $10^{20}$ cm$^{-3}$ or larger, it has become possible with epitaxial growth techniques and novel nitrogen sources to reduce the carrier concentration to the $10^{17}$ cm$^{-3}$ level.

In ScN the conduction band has essentially a Sc 3*d* character. Sc donates its two 4*s* and single 3*d* electrons to the nitrogen and in that sense behaves essentially like an ordinary group-III element. The dispersion of the empty *d* bands in ScN however leads to an indirect band gap with the conduction band minimum at the *X* point of the Brillouin zone.[10] Although one might at first have thought that Mn doping will simply start filling the conduction band in a rigid band picture, we show that the Mn *d* states in Mn-doped ScN instead form localized levels in the gap.

## II. COMPUTATIONAL METHOD

We use the density functional method[11] in the local spin density approximation[12] in conjunction with a supercell approach and the linearized muffin-tin orbital (LMTO) band structure method.[13] We have used the LMTO method both in the atomic sphere approximation (ASA) and in a full-potential (FP) implementation.[14] ASA is adequate as long as we consider highly symmetric crystal structures with sufficiently good sphere packing. As usual empty spheres are added in ASA to improve the sphere packing whereas in FP-LMTO these are not needed. A double basis set with optimized basis functions is used in the FP-LMTO approach. Convergence of the Brillouin zone integrations using a $6\times6\times6$ *k*-point mesh as well as the basis set choice were carefully checked. The main reason for using the ASA method is that it allows in a straightforward manner to empirically shift diagonal elements in the Hamiltonian, thereby allowing us to correct the LDA underestimae of the band gap.

 

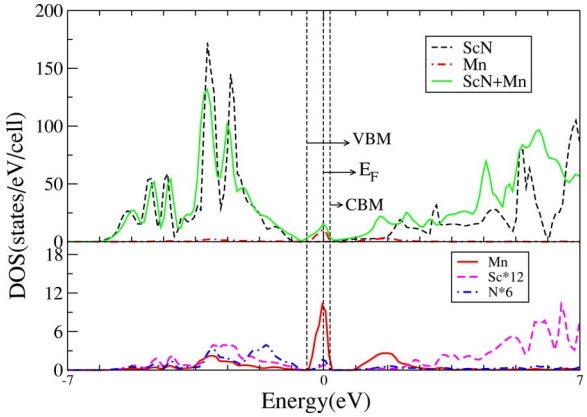


FIG. 1. (Color online) Top: Density of states for pure ScN (black dashed line) and ScN:Mn (green solid line) and partial density of states on Mn $d$ (red dash-dotted line). The vertical lines indicate the valence band maximum, conduction band minimum, and Fermi level. Bottom: various PDOS.

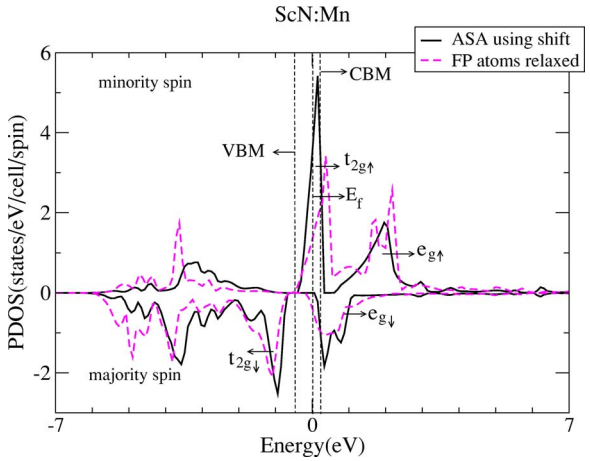


FIG. 2. (Color online) Partial density of states on Mn $d$ in ferromagnetic ScN:Mn: (black) solid line ASA, (purple) dashed line FP.

## III. RESULTS AND DISCUSSION

### A. Magnetic moment and the type of interaction

In LDA calculations ScN comes out to be a zero gap semiconductor due to the usual LDA underestimate of the band gap. Thus to model semiconducting ScN in LDA we need to add a gap correction. Empirically this can be done by adding a small upward shift to the Sc 3$d$ bands which form the lowest conduction bands. Since the valence bands are predominantly N 2$p$ like this does not affect the total energies or the valence bands. This correction can be implemented straightforwardly in the ASA-LMTO method. Justification of this approach in terms of a quasiparticle approach was given in Ref. 10. The so-called screened exchange (SX) and exact exchange (EXX) methods also showed ScN to be semiconducting.[15,16] Furthermore, however, we will show that the main conclusions on Mn doping and its induced magnetism are independent of this gap correction and are maintained in the FP-LMTO results.

We first carried out ASA calculations for a 64 atom supercell of rocksalt ScN doped with a single Mn atom on a Sc site. We include $d$ band shifts on the Sc but not on the Mn because the Mn $d$ states will be at least partially occupied and should not be subject to the upward quasiparticle shifts which only should occur for empty conduction band states. The non-spin-polarized density of states of this system compared with that of the corresponding pure ScN 64 atom supercell is shown in Fig. 1 and clearly shows the presence of a partially filled peak in the gap. We also show superposed in this figure the partial density of states (PDOS) projected on the Mn $d$ orbitals. The PDOS of Mn $d$ and the neighboring atoms are also shown in the bottom panel of that figure for better clarity. This shows that the state in the gap is strongly localized on Mn. We can see a part of the PDOS on Mn is also overlapping with the N 2$p$ valence and Sc 3$d$ conduction bands, indicating bonding with N. Having now a large density of states at the Fermi level, pinned at this Mn level, we may expect that the Stoner criterion for formation of a magnetic moment will be fulfilled. Or, in an alternative view, in such a localized level, Hund's rule will favor a high-spin state.

A spin-polarized calculation shows that indeed a spin splitting of this level occurs. The partial density of states on Mn for the two spin channels is shown in Fig. 2. Further decomposition of the PDOS in specific orbital contributions reveals that the sharp peak at the Fermi level has predominantly $t_{2g}$ character. The dominant orbital character of the peaks is indicated in Fig. 2. As expected, the $e_g$ orbitals $d_{x^2-y^2}$ and $d_{3z^2-r^2}$, which point directly toward the N, form bonding (predominantly N 2$p$ like) states and antibonding (predominantly Mn $e_g$ like states). The $t_{2g}$ states form weaker $\pi$ bonds with N 2$p$. The calculation gives a net magnetic moment of 2.1 $\mu_B$. The following idealized model rationalizes this result. In forming the bonds with N we may assume that Mn donates its two $s$ electrons and one $d$ electron to N (in an idealized ionic trivalent picture) and is therefore in a $d^4$ configuration. A net magnetic moment of 2 $\mu_B$ indicates that the $e_g - t_{2g}$ splitting is larger than the spin splitting, thus leading to a configuration $t_{2g\downarrow}^3 t_{2g\uparrow}^1$. In reality, because of broadening of the levels into bands, the $e_g$ states also contribute partially to the Mn-induced states and lead to a slightly larger magnetic moment.

FP-LMTO calculations including structural relaxation around the Mn (but without $d$-band shift) confirm this picture except that now the Mn $d$ states are resonant with the low density of states bottom part of the Sc 3$d$-like conduction band of states as shown in the dashed lines of Fig. 2. A slightly larger magnetic moment of 2.5 $\mu_B$ is obtained with a 0.5 $\mu_B$ contribution from the $e_g$ states. The structure is relaxed by moving the N 0.12 Å closer to the Mn atom. Thus, although the ASA and FP calculations do not exactly agree with each other in the values of the magnetic moment, the essential picture is the same: a sharp level is associated with the Mn states and becomes spin split. In reality, including gap corrections as we modeled in the ASA, this level can be expected to occur in the gap while in our uncorrected FP calculation, it occurs slightly above the conduction band minimum. Nevertheless for the purpose of calculating total energy differences, we will below focus on results obtained within the FP-LMTO method.

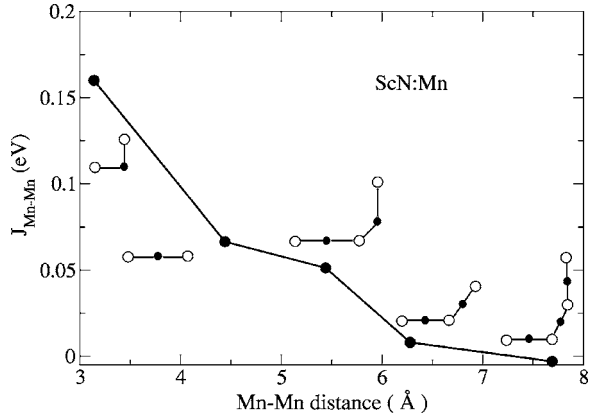


FIG. 3. Near neighbor Mn-Mn exchange interactions as function of distance in ScN:Mn.

As the next step, we carried out FP-LMTO calculations with two neighboring Mn in a 64 atom supercell at different distances from each other and calculate their energy difference for antiparallel spin or parallel spin. This energy difference can be mapped to a Heisenberg Hamiltonian

$$H = -\sum_{\langle ij \rangle} J_{ij} \mathbf{S}_i \cdot \mathbf{S}_j. \tag{1}$$

We find the FM configuration to have lower energy than the AFM configuration by 320, 133, 102.5, and 16 meV, respectively, for first through fourth nearest neighbor pair of Mn. Since these supercells contain, respectively, 1, 2, 2, and 4 Mn-pair interactions per cell, the $E_{\mathrm{AF}}-E_{\mathrm{F}}$ correspond, respectively, to $2J_1$, $4J_2$, $4J_3$, and $8J_4$. The fifth nearest neighbors fall outside the supercell and the sixth neighbor interaction was found to be antiferromagnetic but negligibly small (−3 meV). We note that his assumes the cell is sufficiently large that we may neglect exchange interactions between one supercell and a neighboring one. We thus obtain the exchange interactions shown in Fig. 3. Similar results were obtained using ASA calculations. The FP and ASA give agreement with each other on these values to within a few meV.

The ferromagnetic coupling even between nearest neighbors is somewhat surprising given that in MnN this coupling is antiferromagnetic. This difference however may be due to the larger Mn-Mn distance which will tend to lead to less overlap between the Mn $t_{2g}$ orbitals, which favors ferromagnetic coupling in view of a Heitler-London-type picture. Also, the exchange interactions here are much stronger than in MnN. They are, however, comparable to exchange interactions reported for other dilute magnetic semiconductor systems. For the in-line Mn-N-Mn second nearest neighbor interaction we can expect that double exchange via N and Mn $e_g$ orbitals contributes significantly to the interaction as was also found to be the case in MnN and $Mn_3N_2$.[17]

The magnetic moments per cell is about 5.8 $\mu_B$ (in FP and for both first and the fourth nearest neighbor configuration) slightly larger than twice the single Mn dopant value of 2.5 $\mu_B$. For the third neighbor it is about 5.5 $\mu_B$. Furthermore for Mn placed as second nearest neighbors the magnetic moment is further enhanced to 5.94 $\mu_B$, i.e., almost 3 $\mu_B$ per Mn, indicating that this configuration is particularly favorable toward ferromagnetic moment formation. We note that in MnN (Ref. 17) the magnetic moment is also about $3\mu_B$.

### B. Solubility of Mn in ScN

Next we examine the prospects for successfully doping Mn into ScN. The energy of formation of the Mn impurity is calculated as

$$\Delta E_f(\mathrm{Mn_{Sc}}) = E_s(\mathrm{Sc_{31}MnN_{32}}) - E_s(\mathrm{Sc_{32}N_{32}}) - \mu_{\mathrm{Mn}} + \mu_{\mathrm{Sc}}, \tag{2}$$

where $E_s$ is the supercell total energy and $\mu_{\mathrm{Mn}}$ and $\mu_{\mathrm{Sc}}$ are the chemical potentials of Mn and Sc, respectively. For these we assumed a reservoir of bulk fcc Sc or Mn. We obtain $\Delta E_f(\mathrm{Mn_{Sc}})=3.7$ eV using the spin-polarized Mn result and fully relaxed FP-LMTO calculations. This value is similar to those for other dopants in magnetic semiconductors. For a supercell with two first through fourth nearest neighbor Mn atoms, we obtain an energy of formation which is higher than twice the single $\mathrm{Mn_{Sc}}$ formation energy by 0.38, 0.23, 0.30, and 0.32 eV, respectively.[18] These results indicate that there is *no tendency for the Mn to cluster*.

Next, we estimate the equilibrium miscibility of this system. The energy of mixing is defined as

$$\Delta H_m(\mathrm{Mn}_x\mathrm{Sc}_{1-x}\mathrm{N}) = E(\mathrm{Mn}_x\mathrm{Sc}_{1-x}\mathrm{N}) - xE(\mathrm{MnN}) - (1-x)E(\mathrm{ScN}). \tag{3}$$

To calculate it for a random alloy we follow a cluster expansion approach.[19] We first calculate $\Delta H_m^n$ for specific structures with the $L1_2$ ($Cu_3Au$ ordering) for 25 and 75 % Mn, and $L1_0$ (CuAu ordering) for 50% each fully relaxed. Along with the pure ScN and pure MnN compounds, these represent the five possible nearest neighbor tetrahedron environments on the fcc cation sublattice. Because for MnN, the (LSDA) calculations underestimate the lattice constant by a few percent in contrast to ScN where the agreement is within less than a percent, we actually use the experimental lattice constant for MnN and we add a corresponding correction to the lattice constants for the mixed compounds in proportion to their Mn content. This avoids overestimating the strain effects due to lattice mismatch between MnN and ScN. From these ordered compound energies, we obtain the energy of the random alloy from

$$\Delta H_m(x) = \sum_{n=1}^{4} \binom{4}{n} x^n (1-x)^{4-n} \Delta H_m^n. \tag{4}$$

The values for the ordered compounds and random alloy are shown in the bottom panel of Fig. 4. Finally, we fit the resulting equation to a parabola $\Delta H_m(x)=\Omega x(1-x)$. Within the regular solution model, the entropy of mixing is given by $\Delta S_m=-k[x\ln x+(1-x)\ln(1-x)]$ and the mixing temperature $T_m(x)$ is give by $dF/dx=0$ or

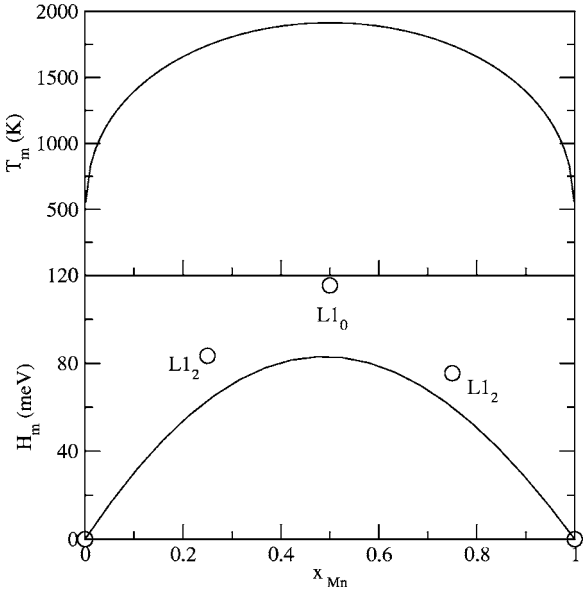


FIG. 4. Mixing energy of $Mn_xSc_{1-x}N$ ordered compounds (circles) and random alloy (solid line) in bottom panel and resulting mixing temperature (top panel) in regular solution theory.

$$T_m(x) = \frac{\Omega}{k}\frac{(1-2x)}{[\ln(1-x) - \ln x]}. \tag{5}$$

With our calculated value of $\Omega = 330$ meV we can solve this equation backward for the miscibility $x$ at a given temperature. At a typical growth temperature of 800 K, we obtain an equilibrium miscibility of only 1%. The miscibility gap temperature, i.e., the temperature above where full miscibility occurs is calculated to be $\Omega/2k \approx 1900$ K. Of course, this should be considered only as a rough estimate because of (1) the use of a mean field theory for estimating the critical temperature, (2) the uncertainties on the convergence of the cluster expansion technique when restricted to nearest neighbor tetrahedrons, (3) the local density approximation which turns out to be less accurate in predicting lattice constants for MnN than ScN, and (4) the fact that small energy differences are obtained from large total energies. Typically, calculations tend to overestimate $T_m$, so we conclude that the equilibrium miscibility could be of order a few percent at the growth temperatures used.

Experimentally, Al-Brithen *et al.*[4] have demonstrated the growth of mixed $Sc_{1-x}Mn_xN$ alloys obeying Vegard's law up to 26%. This however probably does not represent the equilibrium solubility because they used molecular beam epitaxy (MBE) which is a nonequilibrium growth method. For comparison, many semiconductor pseudobinary alloys such as $Ga_xIn_{1-x}N$ which also share the same crystal structure and have similar lattice mismatches between the end compounds have even larger miscibility gap temperatures and lower equilibrium solubilities. Nevertheless mixed compounds up to concentrations of 30% can be obtained in MBE growth. Complete phase segregation does not occur, although some fluctuations in In concentration have been observed and widely discussed. It shows that for practical purposes mixed alloys of $Sc_{1-x}Mn_xN$ can be obtained up to much larger concentrations than for example for GaAs:Mn where around 10% Mn pure MnAs starts precipitating.

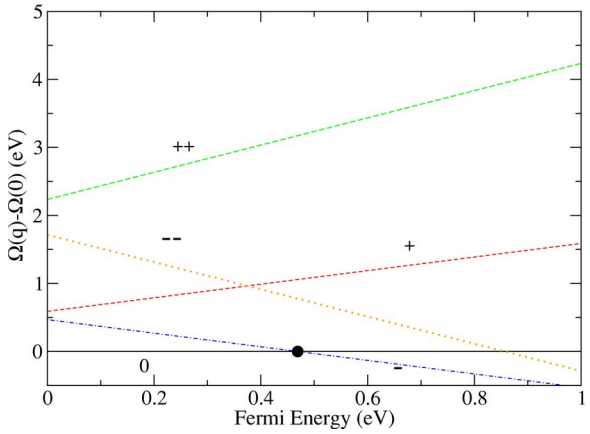


FIG. 5. (Color online) Energy of formation for different charge states as function of Fermi energy in ScN:Mn.

### C. Rough estimate of Curie temperature

To make a first rough estimate of the Curie temperature, we calculate the total exchange parameter

$$J_0 = \sum_R p_R(x,T)J(R), \tag{6}$$

with $x$ the concentration of Mn and $p_R(x)$ the probability that a given neighbor site is actually occupied by Mn. Assuming random distribution because of the absence of any clustering $p_R(x,T) = x$ and we obtain $J_0/x = 3.65$ eV. Assuming a classical Heisenberg model is applicable, $T_c$ should then be of order

$$T_c = \frac{1}{3k}J_0. \tag{7}$$

This gives about 424 K for 3% of Mn. We caution that the validity of the mean-field approximation for dilute magnetic semiconductors is rather doubtful. Local environment effects related to the randomness and percolation effects are expected to play a significant role.[20–23] Nevertheless, our calculations already indicate that this is a promising system with fairly long range and strong nearest neighbor exchange interactions. The higher miscibility should allow more flexibility than in other magnetic semiconductor systems.

It is noteworthy that this ferromagnetic coupling occurs even though Mn does not dope ScN $p$ type. The Mn induced states lie in the middle of the band gap and form deep levels. In all of the above we have assumed the defect level to be in the neutral state. In other words, the ferromagnetism predicted here *is not due to mobile carrier induced coupling*. Rather we have local magnetic interactions.

### D. Charged states and effects of *n*-type doping

The total energy of various charge states for $Mn_{Sc}$ are shown in Fig. 5 as a function of Fermi energy. In this case, the energy of formation in Eq. (2) contains an extra term

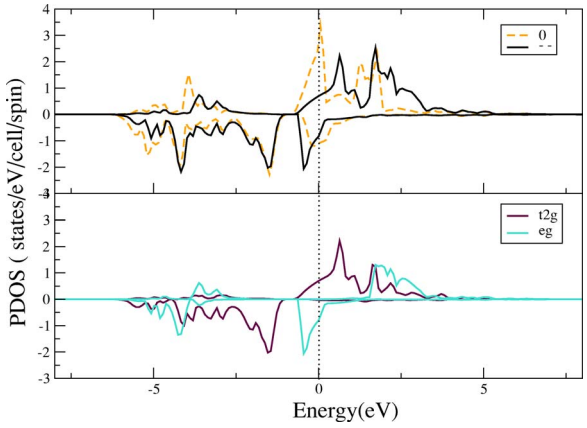


FIG. 6. (Color online) Top: PDOS are compared for neutral (orange dashed line) and double negative charge (black solid) state of ScN:Mn. The vertical dashed line is the Fermi energy picked as zero. Bottom: shows the $t_{2g}$ $e_g$ contributions in case of the double negative charge state.

$q(E_{vbm}+E_F)$ and we also add a correction for the spurious interaction of the periodic array of point charges with the neutralizing background.[8] Using the simple estimate proposed by Blöchl[9] this correction is given by $E_{\mathrm{cor}}=(9/5)q^2/\epsilon R$ where $R$ is the radius of a sphere with the same volume as the supercell $V_{\mathrm{cell}}=4\pi R^3/3$ and Rydberg atomic units are used. The static dielectric constant for ScN has not been measured to the best of our knowledge but we used an estimated value of $\epsilon=8$ based on the ratio of the static to dynamic values in GaN and the calculated value of the high-frequency dielectric constant of 4.4.[10] One can see that the $0/-$ transition state occurs at 0.47 eV, in good agreement with the position of the defect level as seen from the density of states plots. It means that the defect is a deep acceptor. The situation is thus similar to that of Mn-doped GaN.

One might expect that $n$-type doping will lead to an increase in the occupation of the minority $t_{2g\uparrow}$ level and will thus reduce the magnetic moment. However, the calculations reveal that for a negative charge state, the $e_g$ majority states increasingly contribute to the magnetic moment while the $t_{2g}$ contribution is reduced. This is illustrated in Fig. 6. The magnetic moment increases to 3.19 $\mu_B$ in the negative charge state. We have not yet studied in detail how the exchange interactions behave as a function of carrier concentration. In any case, we may safely conclude that $n$-type doping does not wipe out the magnetic effects and since the couplings obtained here were not based on a carrier induced mechanism because the Mn induced acceptor level is deep in the gap, they are also expected to survive. In fact, $n$-type doping may lead to additional long-range carrier mediated couplings between the Mn induced magnetic moments.

ScN is usually unintentionally $n$-type either because of nitrogen vacancies or oxygen impurities. The presence of local magnetic moments on Mn may be expected to result in a small spin splitting of the Sc $3d$-like conduction bands. In a band structure plot of the 64-atom cell, we can identify the Sc conduction bands and these show indeed a spin splitting of about 0.3 eV. This may be expected to lead to interesting effects on the carrier transport, similar to those observed in $Er_xSc_{1-x}As$ which is paramagnetic [or antiferromagnetic (AFM) at low temperature] but nevertheless shows interesting spintronic behavior in an external magnetic field,[24–27] such as a beating of the Shubnikov-deHaas magnetoresistance signal or a spin-dependent resonant tunneling.

A $n$-type ferromagnetic semiconductor is advantageous for spintronic applications requiring a long spin lifetime. In fact, the conduction band minima at the $X$ points of ScN are not degenerate (besides, of course, the degeneracy between the three equivalent $X$ points) and thus should essentially not be subject to any spin-orbit coupling effects. Except for possible mixing among the different valleys, which is usually neglected in calculating spin-relaxation times,[28] spin-orbit coupling effects should be absent in contrast to spintronics based on holes in the valence band maximum at $\Gamma$. This is favorable to avoid spin flipping. Finally, we note that ScN is closely lattice matched to GaN and thus Mn-doped ScN may also serve as a good spin injector into GaN.

## IV. CONCLUSION

In summary, the present computational study predicts that Mn doping in ScN would lead to localized magnetic moments of about 2–3 $\mu_B$ on Mn which couple ferromagnetically up to at least fourth nearest neighbors even in the absence of any carrier induced coupling and may lead to above room temperature $T_c$ for readily achievable Mn concentrations. A small amount of $n$-type doping, which is usually unintentionally present in ScN, will lead to carriers which undergo a sizable spin splitting and hence would be useful for spintronic applications. Two significant advantages of this magnetic semiconductor are pointed out: a reasonably large solubility of Mn in ScN due to their common crystal structure and the fact that this is a $n$-type semiconductor which should reduce spin-orbit coupling induced spin-flip scattering.

## ACKNOWLEDGMENT

This work was supported by the National Science Foundation under Grant No. ECS-0223634.

[1] K. W. Edmonds, K. Y. Wang, R. P. Campion, A. C. Neumann, N. R. S. Farley, B. L. Gallagher, and C. T. Foxon, Appl. Phys. Lett. **81**, 4991 (2002); B. L. Gallagher, Bull. Am. Phys. Soc. **50**, 160, abstract B10.00004 (2005).

[2] A. Leineweber, R. Niewa, H. Jacobs, and W. Kockelmann, J. Mater. Chem. **10**, 2827 (2000).

[3] MnN is actually found to prefer zincblende structure in recent calculations but is stabilized in a rocksaltlike phase by small

amounts of nitrogen vacancies, as reported in W. R. L. Lambrecht and P. Lukashev, J. Appl. Phys. **97**, 10D306 (2005).
[4] H. A. Al-Brithen, H. Yang, and A. R. Smith, J. Appl. Phys. **96**, 3787 (2004).
[5] G. Travaglini, F. Marabelli, R. Monnier, E. Kaldis, and P. Wachter, Phys. Rev. B **34**, 3876 (1986).
[6] T. D. Moustakas, R. J. Molnar, and J. P. Dismukes, Electrochem. Soc. Proc. **96-11**, 197 (1996).
[7] H. Al-Brithen and A. R. Smith, Appl. Phys. Lett. **77**, 2485 (2000); A. R. Smith, H. A. H. Al-Brithen, D. C. Ingram, and D. Gall, J. Appl. Phys. **90**, 1809–1816 (2001).
[8] G. Makov and M. C. Payne, Phys. Rev. B **51**, 4014 (1994).
[9] P. E. Blöchl, J. Chem. Phys. **103**, 7422 (1995).
[10] W. R. L. Lambrecht, Phys. Rev. B **62**, 13538 (2000).
[11] P. Hohenberg and W. Kohn, Phys. Rev. **136**, B864 (1964); W. Kohn and L. J. Sham, Phys. Rev. **140**, A1133 (1965).
[12] U. von Barth and L. Hedin, J. Phys. C **5**, 2064 (1972).
[13] O. K. Andersen, Phys. Rev. B **12**, 3060 (1972); O. K. Andersen, T. Saha-Dasgupta, R. W. Tank, C. Arcangeli, O. Jepsen, and G. Krier, in *Electronic Structure and Physical Properties of Solids, The Uses of the LMTO Method*, edited by H. Dreyssé, Lecture Notes in Physics (Springer, Berlin, 2000), p. 3.
[14] M. Methfessel, M. van Schilfgaarde, and R. A. Casali, in *Electronic Structure and Physical Properties of Solids, The Uses of the LMTO Method*, edited by Hugues Dreyssé, Springer Lecture Notes, Workshop Mont Saint Odille, France, 1998 (Springer, Berlin, 2000), pp. 114–147.
[15] C. Stampfl, W. Mannstadt, R. Asahi, and A. J. Freeman, Phys. Rev. B **63**, 155106 (2001).
[16] D. Gall, M. Städele, K. Järrendahl, I. Petrov, P. Desjardins, R. T. Haasch, T. -Y. Lee, and J. E. Greene, Phys. Rev. B **63**, 125119 (2001).
[17] W. R. L. Lambrecht, M. Prikhodko, and M. S. Miao, Phys. Rev. B **68**, 174411 (2003).
[18] The atomic relaxation effects are significant on these results. MnN and ScN differ in lattice constant by about 6%. An inward relaxation of N toward the Mn by 0.54 Å occurs and lowers the energy by about 2 eV per Mn.
[19] J. W. D. Connolly and A. R. Williams, Phys. Rev. B **27**, 5169 (1983).
[20] L. Bergqvist, O. Eriksson, J. Kudrnovský, V. Drchal, P. Korhavyi, and I. Turek, Phys. Rev. Lett. **93**, 137202 (2004).
[21] K. Sato, W. Schweika, P. H. Dederichs, and H. Katayama-Yoshida, Phys. Rev. B **70**, 201202(R) (2004).
[22] G. Bouzerar, T. Ziman, and J. Kudrnovský, Europhys. Lett. **69**, 812 (2005).
[23] J. L. Xu, M. van Schilfgaarde, and G. D. Samolyuk, Phys. Rev. Lett. **94**, 097201 (2005).
[24] S. J. Allen, N. Tabatabaie, C. J. Palsmstrom, G. W. Hull, T. Sands, F. DeRosa, H. L. Gilchrist, and K. C. Garrison, Phys. Rev. Lett. **62**, 2309 (1989); S. J. Allen, Jr. F. DeRosa, C. J. Palmstrøm, and Z. Zrenner, Phys. Rev. B **43**, 9599 (1991).
[25] A. G. Petukhov, W. R. L. Lambrecht, and B. Segall, Phys. Rev. B **50**, 7800 (1994); A. G. Petukhov, W. R. L. Lambrecht, and B. Segall, *ibid.* **53**, 3646 (1996).
[26] D. E. Brehmer, K. Zhang, C. J. Schwarz, S. -P. Chau, S. J. Allen, Jr., J. P. Ibbetson, J. P. Zhang, C. J. Palmstrøm, and B. Wilkens, Appl. Phys. Lett. **67**, 1268 (1995).
[27] W. R. L. Lambrecht, B. Segall, A. G. Petukhov, R. Bogaerts, and F. Herlach, Phys. Rev. B **55**, 9239 (1997).
[28] R. J. Elliott, Phys. Rev. **96**, 266 (1954).